# Discover Civil Engineering

Research

# An experimental study of the relationship between modulus of elasticity, Poisson's ratio, and the mechanical properties of high-performance concrete

Bajirao V. Mane[1,2] · Ajit N. Patil[1]

## Abstract
This study investigated the mechanical properties of high-performance concrete (HPC) with the percentage of mineral admixtures. HPC is a good choice for multi-story buildings because it has many advantages. As HPC becomes more popular, it is important to research its properties. This study used the P.C. Aitcin method to design HPC mixes with compressive strengths of 60 to 80 MPa. Fly ash is used for M60 and M70 grade HPC and Silica Fume is used for M80 grade HPC is used as mineral admixture as a 20% replacement for cement. In this research paper, the study of properties of the different ingredients used to make HPC is carried out. The testing of three concrete mixes for mechanical properties such as compressive strength, split tensile strength, modulus of elasticity, and flexural strength, as well as other important properties is done. This study explores High-Performance Concrete (HPC) by precisely controlling the water-to-cement ratio and incorporating mineral and chemical admixtures, achieving strengths from 60 to 80 MPa. It investigates key mechanical properties, establishes empirical equations, and compares findings with codes and literature. The results showed that a lower water-to-binder ratio (w/b) led to better mechanical properties. The experimental program includes the casting of 39 cubes, 39 cylinders, 39 beams and 81 columns to test the physical properties of different concrete grades. The use of a compression testing machine with a load capacity of 3000 kN to test the HPC cubes and a loading frame with a load capacity of 2000 kN to test the columns. The average compressive strength for HPC M60 to M80 was 65.40 MPa, 73.45 MPa, and 82.64 MPa respectively. The modulus of elasticity values ranged from 40 to 50 GPa. The findings of the study showed that an increase in concrete strength correlated with a decrease in the average value of Poisson's ratio. Overall, the study suggests that HPC is a good choice for high-rise buildings because it has many advantages. As HPC becomes more popular, it is important to research its mechanical properties. This study provides valuable results about the mechanical properties of HPC in comparison with IS 456:2000. From the experimental results of tested columns, it was observed that as the load increased, the deflection decreased for both uniaxially and biaxially loaded columns, highlighting the novelty of this finding. Additionally, the columns subjected to biaxial loading displayed greater sensitivity compared to their axial and uniaxial loading.

Keywords  High-performance concrete · Compressive strength · Flexural strength · Split tensile strength · Elastic modulus · Poisson's ratio

---

✉ Bajirao V. Mane, bajimane9090@gmail.com; Ajit N. Patil, ajit.patil@dyptc.edu.in; ajitpatil2525@gmail.com | [1]Department of Civil Engineering, School of Engineering and Technology, DYPU, Ambi, Pune 410506, India. [2]Department of Civil Engineering, Annasaheb Dange College of Engineering and Technology, Ashta, Sangli 416301, India.

Discover

# 1 Introduction

Investigation into HPC is mainly focused on various three areas. The primary area gives detailed investigations of the basic structure of HPC materials [33]. The components of concrete together including the moment interaction between them investigate the properties of the ensuing material. A phenomenon mentioned on the micro-scale, such as hydration of the cement, micropores content along with interface effect among cement pastes along with aggregates, help to understand together including the factors that make the material strength to develop [30]. Studying engineering properties of high-performance concrete constitute another area of research, which includes, Poisson's ratio, compressive strength, ultimate tensile strength along with elastic modulus [29]. The third investigation area is related to the properties of HPC which impacts the behaviour of the structure. The point of interest is given on HPC along with its impacts on distinct strengthened concrete elements inclusive of columns [9]. The research study focuses mainly on the third category of the behaviour of reinforced log columns, with the main emphasis on design-related studies. Some part of the study is also lined with different physical properties of HPC. At present due to taking less space and saving in materials in columns of high-rise structures along with bridges, the use of HPC is increasing [1, 2]. However, more important the value for the strength of concrete motivates designers to minimise the cross-section of structural elements considering the same ultimate strength of the section and along with the slenderness ratio of the reinforced long column is increased [3]. As the usage of HPC increases in popularity, the need of research in providing technical details on this new material becomes prominent [14]. The use of high-performance concrete (HPC) in the construction of high-rise structures gives significant benefits that justify investigation as a cost-effective and attractive choice [10, 11]. The development of HSC is attributed to Yoshida, who used high-strength compaction to create concrete with a strength greater than 96 MPa. HPC gives special performance along with consistency desires that can't always be achieve habitually using regular materials and standard mixing, placing and curing practices. Today, high strength long RC columns have become more and more accepted in the construction business [37]. Such concrete cannot be high strength concrete or concrete with standard strength. All countries economic health is now determined by the structures long-term functionality. Concrete has been a fundamental component of dependable infrastructure construction since the Greek and Roman eras. When taken as a whole, the decision to incorporate high-performance concrete into high-rise building designs has several advantages, making it a prudent decision from an aesthetic and economic perspective. All things considered, using HPC for high-rise structures has enough benefits to merit consideration as an appealing and affordable alternative. Once HPC is widely available, the need of research contributions in providing appropriate recommendations on this new concrete material becomes evident.

According to ACI-3184, the value of the gradient of the chord made between the origin and the location on the curve that corresponds to 45% of the mean compressive strength of cylinders may be used to determine the elastic modulus of concrete. Multiple researchers have utilised this value in their articles, including [7]. Other writers, namely [15], and certain standards (such as Australian Standard AS 1012, Erocode-2, and ASTM C469) accept an explanation that is similar but places the reference point at 40% of the strength. The definition of the elastic modulus of high strength concrete, as determined by some of the early researchers in the field, was associated with the tangent slope of the stress–strain curve at 25% of maximum stress. Furthermore, the chord's slope at 60% of the peak was suggested by Thorenfeldt, Tomasiewicz et al. 1987 as an additional elastic constant.

The following formula, which is established in accordance with ASTM C4697 at 40% of the ultimate load, was presented for the static modulus of elasticity of high strength concrete.

$$Ec = 3320\sqrt{f'_c} + 6900 \, (MPa) \tag{1.1}$$

The strength range between 21 and 83 MPa is represented by the preceding equation. With the following formula, this equation tried to rectify the ACI-3184 estimation for concrete of normal strength.

$$Ec = 4730\sqrt{f'_c} \, (MPa) \tag{1.2}$$

## 1.1 Research significance

The significance of this research lies in its thorough exploration of the mechanical properties of high-performance concrete (HPC) with use mineral admixtures. In response to the growing popularity of HPC, especially in multi-story buildings, the study

utilizes the P.C. Aitcin method to design mixes with compressive strengths ranging from 60 to 80 MPa. By incorporating fly ash and silica fume as mineral admixtures, the research investigates the properties of different HPC ingredients, conducting extensive testing for compressive strength, split tensile strength, modulus of elasticity, and flexural strength. The study's innovative approach, including empirical equations and comparisons with industry standards, contributes valuable insights to the optimization of HPC's mechanical properties, reinforcing its suitability for high-rise structures.

Bridges, buildings, and other structures currently make extensive use of HPC. However, existing codes, like IS 45621, primarily depend their design requirements for reinforced concrete components on empirical relationships for mechanical characteristics derived by testing normal strength concrete and the associated statistical parameters. This raises the possibility that when NSC-developed equations are used in HPC, the design may not be conservative. However, the equations can be excessively conservative, which would limit the benefits of utilising HPC. Therefore, studies are required to establish a statistically significant association between splitting tensile strength (fsp), modulus of rupture (fr), and modulus of elasticity (Ec) and the stipulated design compressive strength of HPC. The novelty of this study lies in its focused investigation of slender reinforced columns utilizing High-Performance Concrete (HPC) in the M60 to M80 strength range and subjected to different loadings. This research extends beyond conventional studies by exploring the complex interaction between high performance concrete, slender column geometry, and different loading conditions.

## 2  Research gap

The French invented the term "High-Performance Concrete" in 1980. In 1986, 36 journals from France, Switzerland, and Canada came together to form the French Initiative for New Concrete Methods. Led by Pierre-Claude Aitcin from Canada, the group published the first book entirely dedicated to High-Performance Concrete research, results, and applications. Aitcin et al [8] built a network of research centres for high-performance computing (HPC) with the help of the government and two colleagues. The network became known as Concrete Canada and began work in 1990. Many studies and publications on HPC were produced between 1990 and 2000. HPC is now a popular area of research in many countries around the world. Many large cities and state highway authorities are using HPC or are planning to use it. As a result, more and more consultants and subcontractors are getting work that involves HPC.

### 2.1  American Association of State Highway and Transportation Officials/American Society for Testing and Materials (AASHTO/ASTM)

In the AASHTO and ASTM codes, conversion coefficients are furnished to assess strength test outcomes in cases where the h/d ratio is below 1.8. These coefficients serve to transform strength test outcomes into commensurate results for specimens with an h/d ratio of 2. Typically, these coefficients find application in tests conducted on cores extracted from structures [17]. The values of these coefficients for varying h/d ratios are detailed in Table 1.

### 2.2  United Nations Educational, Scientific and Cultural Organization (UNESCO)

The UNESCO manual on reinforced concrete offers conversion coefficients tailored to specimens of different dimensions and configurations [23]. The conversion factors suggested by UNESCO are outlined in Table 2.

### 2.3  Naville's equation

In 1966, Naville synthesized data from numerous prior investigations to formulate a comprehensive correlation encompassing compression test specimens of diverse shapes and dimensions. The resulting relationship, as presented below, was documented [31].

| Table 1  Values of factor as per AASHTO/ASTM | | | | |
|---|---|---|---|---|
| *h/d* | 1.75 | 1.5 | 1.25 | 1.00 |
| Factor | 0.98 | 0.96 | 0.93 | 0.87 |

**Table 2** Factors recommended by UNESCO

| Specimen Shape | Specimen Size in mm x mm | Conversion factor |
|---|---|---|
| Cylinder | $150 \times 300$ | 1.00 |
| | $100 \times 200$ | 0.97 |
| | $250 \times 500$ | 1.05 |
| Cube | $100 \times 100 \times 100$ | 0.80 |
| | $150 \times 150 \times 150$ | 0.80 |
| | $200 \times 200 \times 200$ | 0.83 |
| | $300 \times 300 \times 300$ | 0.9 |

$$\frac{P}{P_6} \times \frac{d}{d_6} = 0.8878 \left( \frac{A}{A_6} \right)^{0.4525} \tag{2.1}$$

Where, $d_6$=A 150 mm cube's greatest lateral dimension$A$=cross-sectional area, and$A_6$=a 150 mm cube's cross-sectional area$P/P_6$=ratio of cylinder strength to cube strength

## 2.4 L'Hermite's equation

Back in 1955, R. L'Hermite put forth a straightforward equation that established the cylinder/cube strength ratio in relation to the cube strength.

$$\frac{Cylinder\ strength}{Cube\ strength} = 0.76 + 0.2 log_{10} \frac{f_{cu}}{2840} \tag{2.2}$$

where $f_{cu}$ cube strength in psi.

The findings of certain researchers in the literature regarding the cylinder to cube ratio are depicted in Table 3.

Examining various techniques is crucial for evaluating the pozzolanic activity of materials, commonly used in construction to improve concrete properties. Pozzolanic materials react with calcium hydroxide to form cementitious compounds. Assessing pozzolanic reactivity is vital for material selection and optimizing concrete mixtures. The combination of direct and indirect testing methods offers a thorough understanding of pozzolanic reactivity. The choice of methods depends on material characteristics and desired concrete properties. Ongoing research and standardization efforts enhance the accuracy and reliability of these testing techniques [18].

The mechanical properties of fiber-reinforced concrete (FRC) at high temperatures have been evaluated using artificial intelligence (AI). The developed information fills in research gaps in fiber-reinforced concrete (FRC), especially for high fibre aspect ratios and content (> 0.8%). It also includes concrete compositions, fibre properties, and temperatures. According to AI models, polypropylene fiber-reinforced concrete (PFRC) loses less residual compressive strength than steel fiber-reinforced concrete (SFRC). At all temperatures, the compressive strength of steel fibre is enhanced by varying its diameters. Additionally, longer polypropylene fibers and higher content contribute to reduced tensile strength degradation. Probabilistic analysis highlights PFRC's consistent failure probability (Pf) at around 50%, while SFRC's Pf is

**Table 3** Some results of cylinder vs. cube comparative studies

| Reference | Average cylinder/cube ratio | Remarks |
|---|---|---|
| Cormack | 0.87 | The research concentrated on high-strength concrete |
| Evans | 0.77–0.96 | Lower strength concretes have a lower cylinder/cube strength ratio in general |
| Lysle and Johansen | 0.86 | – |
| Gonnerman | 0.85–0.88 | Standard cylinders of 150 mm × 200 mm were used in the tests |

lower for water-to-binder ratios between 0.4 and 0.5. Notably, Pf for both fibers at a W/B ratio of 0.5 is relatively constant. The critical temperature for failure is 550 ℃ for SFRC and 430 ℃ for PFRC [19].

A comprehensive review of previous research reveals that high-strength concrete is significantly more brittle than traditional normal-strength concrete. This is because strength and ductility are inversely correlated. As a result, concrete confinement is essential for high-strength concrete columns. However, there is a scarcity of published data on large-scale high-strength concrete reinforced concrete structures above 80 MPa [26].

The present study includes a thorough assessment of various reinforced concrete components as well as the determination of fundamental mechanical properties like compressive strength, tensile strength, and elastic modulus. The formulation of equations for various parameters will be presented, followed by a comparison with already-formulated equations. The failure patterns of concrete cubes and cylinders of conventional strength will be compared to those of concrete of higher strength. In addition, possible differences between the failure patterns shown by cubes and cylinders may be analyzed.

## 3  Methodology

Mix proportion is the procedure of evaluating the right combination of ingredients to prepare a homogeneous cement concrete mix with the required properties at a very low probable cost. Although regular normal concrete, the progression is cumbersome as various conflicting requirements must be balanced.

### 3.1  Selection of ingredients for HPC

HPC manufacturing is a more complex process than normal concrete due to a number of parameters to be managed to become more important two mineral admixtures and superplasticizers. It is required to have bond between cement and superplasticizer so that they form a liquid mixture and remain in liquid form for a long period to place easily. Throughout the entire examination, OPC of 53 grades (Ultratech cement), which is commercially available and confirms relevant IS code (IS 12269-1987), was used. Improved strength development functionality Cement grades 43 and 53, which conform to IS 8112-1989 and IS 12269-1987, respectively, are now available in India. Depending upon the strength and durability necessities the sort of cement can be selected to achieve economy in the mix proportions. In this experimental research crushed basalt stone in the form of small pieces are used as coarse aggregates.

The maximum size of aggregate was 20 mm down to produce 60 Mega Pascal and 12 mm down for 70 Mega Pascal to 80 Mega Pascal. Sand mixed stock that passes through a 75-micron sieve and have a silt content by weight are considered to be silt. This silt makes concrete less workable, increases the W/C ratio, and decreases strength. Sand available from Krishna River was used for entire testing. The sand that was applied fits into grading zone III of Table 4 IS:383-1970. Elkem material were provided the silica fume and fly ash which required for this experimental work. Micro silica is one in every of the goods furnished by resources of Elkem materials.

To keep the required workability of HPC, the water content will be reduced using superplasticizers. Master Glenium Sky 8654 is use as a strong water reducer. This is where Glenium B233 differs from conventional super plasticizers. so far, they have been mostly based on unique carboxylic ether polymers with long polymer chains. What differentiates Glenium products apart from traditional super plasticizers is a new, unique mechanism of action that significantly progress the effectiveness of distribution.

Customary superplasticizers based entirely on melamine and naphthalene suffocates are polymers that can be absorbed through cement granules. According to IS 456–2000 article 4.3, water added for mixing of concrete and used for curing purposes must be free from potentially harmful substances. Uses potable water with a pH of between 7 and 7.5. The clause also stipulates that the pH level cannot be lower than 6. In this study, the only potable tap water available in the lab was used. After carefully considering the literature suggestions and conducting an analysis, we have opted to utilize HPC ingredients that fulfil the required properties. Based on that Table No. 4 shows the properties of selected ingredients.

#### 3.1.1  Specimens

The cubes (150 mm × 150 mm × 150 mm) and cylinders (150 mm × 300 mm) were used to determine the required compressive strength. The split tensile strength was measured on 150 mm by 300 mm cylindrical specimens. We measured the

**Table 4** Materials used with their properties

| Cement | |
|---|---|
| Grade of Cement | OPC, 53 Grade, Ultratech |
| Specific gravity of cement | 3.15 |
| Coarse Aggregates (CA) | |
| Specific Gravity of CA | 2.95 |
| Maximum and Minimum size of CA | 16 mm & 10 mm |
| Impact Value of CA | 18.60% |
| Water Absorption | 2.52% |
| Bulk Density of CA | 2087 kg/m$^3$ |
| Crushing Value of CA | 16.70% |
| Fine Aggregates (FA) | |
| Specific Gravity of FA | 2.88 |
| Bulk Density of FA | 1640 kg/m$^3$ |
| Silt Content | 3.75% |
| Water Absorption | 3.55% |
| Fineness Modulus of FA | 2.60 |
| Superplasticizer | |
| Brand Name | Master Glenium Sky 8654 |
| Specific Gravity | 1.10 |
| Producer Company | BASF |
| Specifications for reference | IS 9103:1999 |
| Solid Content | 33% |
| Silica Fume (SF) | |
| Specific Gravity SF | 2.15 |
| Fly Ash | |
| Specific Gravity Fly Ash | 2.10 |
| Consumable Water | |
| P$^H$ | 7.0–7.6 |

flexural tensile strength of 100 mm × 100 mm × 500 mm beams. Cylinders measuring 150 mm by 300 mm were tested in order to investigate the stress–strain relationship and elastic modulus. The material properties are as shown into Table 4.

## 3.2 Design mix of HPC from M60 to M80

HPC shows very low porosity and the strongest transition zone results in great durability and strength characteristics. In HPC, minimizing water content from the concrete also maintaining the required workability is prime important and is achieved by adding superplasticizers. using the method suggested by Aitcin et al. 1998, the concrete of strengths 60 Mega Pascal to 80 Mega Pascal were produced by using ingredients like fine aggregates (locally available river sand), coarse aggregates (crushed stone chips), OPC cement of 53 grade, mineral admixtures (Fly ash and Silica fume) and superplasticizer (Master Glenium 233). Water cement ratio is different according to the concern of workability for M60 to M80, to maintain proper workability for the design mix the percentage of superplasticizer is different for each grade. outliers in the analysis of high-performance concrete (HPC) can distort key properties such as compressive strength, workability, and durability. Proper identification and handling of outliers are crucial to ensure accurate assessments of HPC performance, influencing aspects like mix design, construction processes, and quality control measures. The Addressed outliers was essential for maintaining the superior mechanical properties associated with high-performance concrete.

The final design mix proportion for 60Mpa to 80Mpa is as shown in Table 5.

Concrete mix design (proportioning) consists of different steps to calculate the desired proportion of required materials which will produce a mixture with the appropriate properties at very minimum possible cost. High-performance concrete is produced with proper selection of different ingredients. To develop and control the rheology of designed concrete, the mechanical and chemical properties of cement are prime important. Water requirements for the consistency of fresh concrete are affected by the fineness of the cement. In HPC, cement strength and bond strength may exceed

**Table 5** Design Mix for HPC M60 to M80

| Materials | Compressive Strength in MPa | | |
|---|---|---|---|
| | 60 | 70 | 80 |
| W/C | 0.44 | 0.39 | 0.36 |
| Cement, kg/m$^3$ | 366 | 405.11 | 441 |
| Fine Aggregate, kg/m$^3$ | 693.24 | 654.90 | 615.78 |
| Coarse Aggregate, kg/m$^3$ | 1087.79 | 1087.79 | 1087.79 |
| Water, kg/m$^3$ | 162.63 | 158.23 | 157.24 |
| Metakaolin, kg/m$^3$ | – | – | – |
| Fly ash or silica fume kg/m$^3$ | 91.42 | 101.29 | 110 |
| HRWR (Master Glenium Sky 8654) in % | 0.4 | 0.42 | 0.45 |

the strength of the aggregates. Hence high strength aggregates used in concrete can lead to a remarkable increase in the strength of concrete. The particle size distribution and shape of particles of fine aggregates are important factors in the manufacturing of HPC. The form and texture of the particles have a considerable impact on the water-cement ratio and compressive strength of the concrete produced. River sand and crushed stones are utilised as fine and coarse aggregates in the production of HPC.

### 3.3 Instrumentation and test set up

A servo-controlled, 3000 kN compression testing apparatus was used to test the cubes and cylinders. A UTM evaluation of the flexural strength was conducted. To monitor longitudinal deformations, LVDTs were mounted on the opposing face of a cylinder. A computer was interfaced with a 12-channel data logger, which was utilised to record load and displacement. Explosive cylinder failure prevented the post peak response of the stress–strain curves from being produced. To guarantee accurate alignment, the top surface of the cylinders was thoroughly ground before they were put in the machine.

## 4  Experimental work

The great difference between traditional cement concrete and HPC is that high-performance concrete consists of mineral admixtures in the matrix. HPC shows very low porosity and the strongest transition zone results in great durability and strength characteristics. In HPC, minimising water content from the concrete also maintaining the required workability is prime important and is achieved by adding superplasticizers. The selected superplasticizers should have more solid content and specific gravity and a longer molecular chain length for better efficiency. The concrete of strengths 60 Mega Pascal to 80 Mega Pascal was produced by using ingredients like fine aggregates (locally available river sand), coarse aggregates (crushed stone chips), OPC cement of 53 grade, mineral admixtures (Fly ash and Silica fume) and superplasticizer (master Glenium 233) using the method suggested by Aitcin. To study the mechanical characteristics of cubes, cylinders, and beams, a Compression Testing Machine (CTM) with a capacity of 3000 kN and a Universal Testing Machine (UTM) with a capacity of 1000 kN are utilised. After 28 days, three tests were performed: flexural strength, split tensile strength, and compressive strength, as shown in Fig. 1.

HPC properties that are equivalent to HSC (high strength concrete) are difficult to believe. The improvement in compressive strength of high-performance concretes is largely dependent on a minimal W/C (water/cement) ratio than on mineral admixtures, such as silica fume, being replaced with cement. The compressive strength will be substantially greater if silica fume content is replaced up to 10 to 15% of cement content. However, the maximum strength gain over high performance concrete is more than 15%. Tables 6, 7 and 8 demonstrate the compressive strength, flexural strength, and split tensile strength of concrete grades M60, M70 and M80 [25, 32].

During the test, the kinds of failure and cracking properties of two types of concrete specimens (cubic and cylindrical) for various concrete mixture strengths were observed. The fracture process can be utilised by a stress concentration at the cube corners in the case of cubes. At the corners, incline micro-cracks appear and become dense. Crushing produces vertical cracks and column-like fragments as the load increases.

**Fig. 1** Testing of cubes and cylinders to access mechanical properties



**Table 6** M60 concrete's compressive strength, split tensile strength, and flexural strength

| Sr. No | Max. Load (kN) | Strength in (N/mm$^2$) | Average strength (N/mm$^2$) | 28 days Strength As per ACI code in N/mm$^2$ | 28 days Strength according IS code in N/mm$^2$ | 28 days Strength according Literature |
|---|---|---|---|---|---|---|
| Compressive strength | | | | | | |
| 1 | 1372 | 60.97 | 61.46 | 70.82 | 60 | 64.06 |
| | 1398 | 62.13 | | | | |
| | 1379 | 61.28 | | | | |
| Flexural Strength | | | | | | |
| 2 | 10.20 | 5.10 | 5.26 | 4.80 | 5.42 | 7.20 |
| | 10.96 | 5.48 | | | | |
| | 10.44 | 5.22 | | | | |
| Split Tensile Strength | | | | | | |
| 3 | 290 | 4.10 | 4.10 | 4.06 | 4.64 | 4.10 |
| | 285 | 4.03 | | | | |
| | 296 | 4.18 | | | | |

**Table 7** M70 concrete's compressive strength, split tensile strength, and flexural strength

| Sr. No | Max. Load (kN) | Strength in (N/mm$^2$) | Average strength (N/mm$^2$) | 28 days Strength As per ACI code in N/mm$^2$ | 28 days Strength according IS code in N/mm$^2$ | 28 days Strength according Literature |
|---|---|---|---|---|---|---|
| Compressive strength | | | | | | |
| 1 | 1610 | 71.55 | 71.35 | 70.82 | 70 | 73.44 |
| | 1630 | 72.44 | | | | |
| | 1577 | 70.08 | | | | |
| Flexural Strength | | | | | | |
| 2 | 11.04 | 5.52 | 5.70 | 5.18 | 5.85 | 5.72 |
| | 11.66 | 5.83 | | | | |
| | 11.51 | 5.75 | | | | |
| Split Tensile Strength | | | | | | |
| 3 | 320 | 4.52 | 4.54 | 4.42 | 5.01 | 4.10 |
| | 327 | 4.62 | | | | |
| | 318 | 4.50 | | | | |

**Table 8** M80 concrete's compressive strength, split tensile strength, and flexural strength

| Sr. No | Max. Load (kN) | Strength in (N/mm²) | Average strength in (N/mm²) | 28 days Strength As per ACI code in (N/mm²) | 28 days Strength according IS code in (N/mm²) | 28 days Strength according Literature |
|---|---|---|---|---|---|---|
| Compressive strength | | | | | | |
| 1 | 1798 | 79.91 | 80.10 | 92.82 | 80 | 88.9 |
| | 1803 | 80.13 | | | | |
| | 1806 | 80.26 | | | | |
| Flexural Strength | | | | | | |
| 2 | 11.96 | 5.98 | 6.01 | 5.54 | 6.26 | 5.60 |
| | 12.10 | 6.05 | | | | |
| | 12.02 | 6.01 | | | | |
| Split Tensile Strength | | | | | | |
| 3 | 341 | 4.82 | 4.83 | 4.76 | 5.36 | 5.40 |
| | 349 | 4.93 | | | | |
| | 336 | 4.75 | | | | |

The first crack in HPC was discovered to form at small stress levels up to 40% of the ultimate load. In HPC, the first cracking occurred at up to 70% of the ultimate load, the number of cracks on against faces developed at around 85%, and the corners ultimately cracked at around 95% of the maximum stress level.

Study of some mechanical properties is also important for design of reinforced concrete members. Based on the experimental data of present study, relation between cylindrical strength and compressive strength of HPC is drafted as shown in Fig. 2. The proposed analytical equations are compared with the equations in the literature and codes and their suitability was discussed. Figure 2. Demonstrates the Relation between cylinder strength and cube compressive strength of HPC ranging from 60 Mega Pascal concrete to 80 Mega Pascal concrete. To access the relation between cylinder strength and cube compressive strength of HPC total 15 samples were casted and tested successfully to propose analytical equations.

It is critical for accurately determining the relationship between concrete cylinder strength and cube strength. However, researchers have tried to relate them analytically and experimentally. The stronger the concrete, the superior the ratio. Figure 3 demonstrates the conversion factor (cylinder-to-cube strength ratio). For the normal strength concrete conversion factor is decided to be 0.8 up to strength 60 Mega Pascal concrete and 0.85 for strength 80 Mega Pascal onwards. Total 39 beams were casted to access the Relation between compressive strength of concrete and split tensile strength of HPC.

**Fig. 2** Relation between cylinder strength and cube compressive strength of HPC
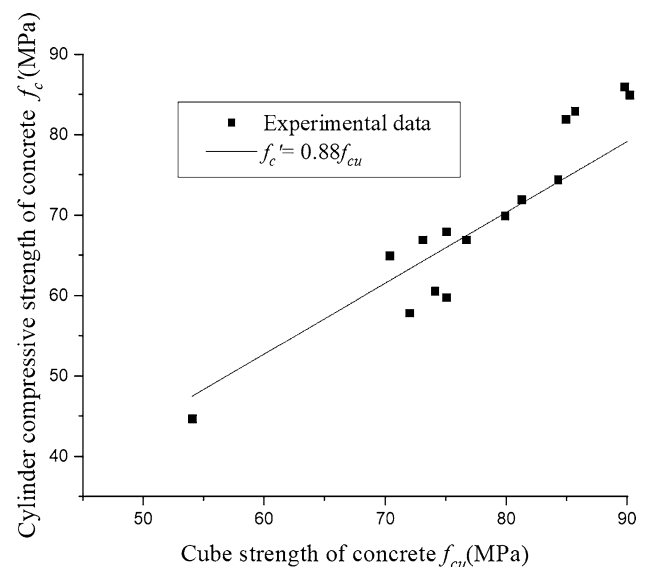
**Fig. 3** Relation between compressive strength of concrete and split tensile strength and error bars to indicate spread of data
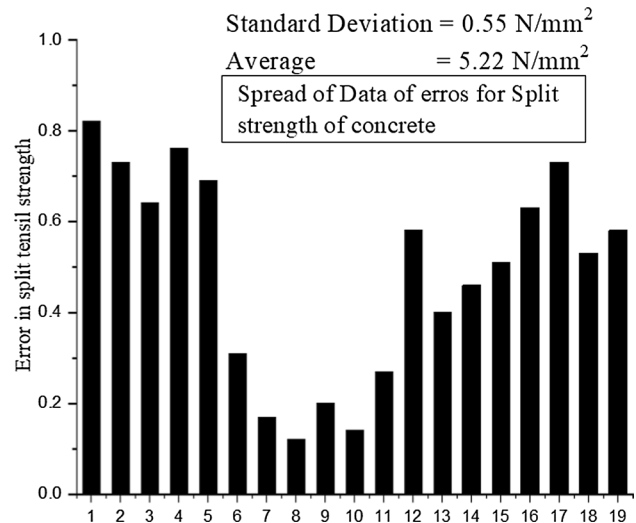


**Fig. 4** Ultimate Cracking pattern of Cubes



A simple inspection indicates that the impact of giving in the specimens was greater in the cubes than in the cylinder. The failure of the cubes and the observed crack pattern is shown in Fig. 4. The inclined fracture surface and diagonal fracture zone for cylinder is as shown in Fig. 5. According to the latest research, the initial crack in HPC cylinders appeared at about 85% of the ultimate stress, but as greater force was applied, the same split failure continued and eventually failed with a smaller number of cracks.

## 5  Result and discussion

The transition zone between the coarse aggregate and the microstructure of HPC is more compact, resulting in either a narrow or non-existent transition zone. Thus, some of the mechanical properties of HPC are influenced by the coarse aggregate. There is a critical value for the water/binder ratio for any coarse aggregate, below which additional reductions in the ratio do not significantly enhance the compressive strength. This crucial value is dependent on both the maximum size of the coarse aggregate and the strength of the rock that is used to make it. This is because, in the process of breaking a specific rock, the tiniest pieces tend to be stronger than the coarsest since they include less failures. The term "size effect phenomenon" is occasionally used to describe this phenomenon.

**Fig. 5** Inclined fracture surface and diagonal fracture zone for cylinder



In general, typical concrete is homogeneous and isotropic, with the hydrated cement paste and/or transition zone acting as the weakest link. However, HPC functions similarly to a non-isotropic composite material composed of aggregates with varying mechanical properties and hydrated cement paste. It appears that the water/binder ratio and the characteristics of each of its parts have an impact on the qualities of this composite material. The test findings and specimens with cylindrical or cubical shapes were used for the compressive test.

## 5.1 Mechanical properties of HPC

For civil engineers and other concrete workers, the mechanical properties of hardened concrete are its most crucial properties. These properties include things like tensile strength, modulus of elasticity, and compressive strength. Since all other concrete strengths, including tensile, flexural, shear, and bond strength, are connected to compressive strength, it is the most important attribute of hardened concrete. Concrete with a high compressive strength will thus have enhanced extra properties.

Concrete's elastic behaviour may be explained by its modulus of elasticity. Because it indicates how much concrete contributes to the flexural stiffness of the member, the modulus of elasticity is important in the design of flexural members. Concrete's stress–strain relationship behaves nonlinearly in the pre-peak zone. As such, figuring out the material's elastic modulus is difficult. There isn't a commonly agreed upon definition because of this. Various codes and researchers used the definition of elastic modulus in relation to chords drawn at different stress levels. ACI 318-08 proposed the chord specified at 45% stress level. Similar concepts are acknowledged by other standards, including Australian Standard AS 101217-1997 [36], Eurocode-2, ASTM C469-87, which puts the reference point at 40% of the strength [20], and other writers for HPC.

It is more likely that before the concrete itself collapses under compression, the tensile strength of concrete structures that collapse with compression will be exceeded. Since it is considered that the reinforcement can bear all tensile stresses, tensile strength is rarely considered throughout the design process. It is believed that the rupture modulus provides the most insight into the flexural behaviour of the members. The results, according to Raphael, are around 50% better than those of the previous two tests. The same source claims that this is the outcome of both an incorrect use of elastic theory to determine the modulus of rupture and the nonlinear characteristics of the stress–strain diagram of concrete under tension [13].

The lateral strain to linear strain ratio in the loading direction is defined as Poisson's ratio. Poisson's ratios range from 0.15 to 0.25. A lower Poisson's ratio indicates brittleness in a greater strength concrete. HPC is currently commonly used in bridges and other constructions. Current code standards for reinforced concrete members, such as the IS 456-2000, are, however, mostly based on empirical relationships obtained through testing normal-strength concrete. When equations created using NSC are applied to HPC members, these highlights relate to that the design may not be appropriate. In contrast, the equations may be excessively sensitive, which leads to the benefits of implementing HPC not being completely utilised. Therefore, additional investigation is required to determine a meaningful relationship between the

associated splitting tensile strength ft, modulus of rupture fr, and modulus of elasticity Ec and HPC's specified design compressive strength (specified design fc').

To comprehensively analyse the mechanical properties of High-Performance Concrete (HPC), one should focus on material characterization, mix design, fresh and hardened concrete properties, durability assessment, microstructural analysis, statistical analysis, and consideration of environmental impact. Tests for compressive strength, tensile strength, modulus of elasticity, workability, durability against permeability, and abrasion should be conducted.

## 5.2 Compressive strength of concrete

It is incorrect to think that HPC's mechanical properties are just those of a more durable concrete. Just as it is incorrect to assert that none of the mechanical characteristics of HPC are related to one another, it is also incorrect to believe that the mechanical properties of HPC may be computed by developing those of ordinary concretes. The microstructure of HPC is more compact, exhibiting a limited or non-existent transition zone, particularly in the transition zone containing coarse aggregate. Consequently, portions of the mechanical properties of HPC are impacted by the coarse aggregate's mechanical characteristics. This is due to the fact that, when a certain rock is crushed, the tiniest bits frequently have fewer cracks and are thus stronger than the coarse aggregate. We refer to this as the "size impact phenomenon."

High Performance Concrete (HPC) and Normal Strength Concrete (NSC) can be broadly classified into the following categories: The transition zone and the hydrated cement paste are usually the weakest points in NSC. NSC is isotropic and homogeneous. It is clear that both the water-to-binder ratio and the elements' characteristics have an impact on this composite material's special attributes.

### 5.2.1 Crack pattern

A key feature of the behaviour of a heterogeneous material such as concrete is microcracking, and the development of microcracking is strongly influenced by the properties of the interfacial transition zone. Because of advancements in the microstructure of concrete, the HPC specimens' mechanism of failure under uni-axial compression is different from that of the NSC specimens. As compressive strength increases, the number and quality of a continuous series of fractures developed during a crack decrease. Cracks in HPC spread throughout the aggregate and paste, reducing resistance throughout the surface area.

After achieving the desired strength of High-Performance Concrete (HPC), as indicated in Tables 7, 8, and 9, the mechanical properties were further evaluated. A total of 39 cubes, 39 cylinders and 39 beams were cast, cured for 28 days, and subsequently subjected to testing. The corresponding test results are summarized in Table 9. So, results from Tables 7 and 8 are little bit different but all results are matches with the characteristic strength.

A stress concentration at the cube corners initiates the fracture process in the case of cubes. As seen in Fig. 6, incline microcracks create and connect within the corners. Crushing produces vertical cracks and column-like material as the load increases, as shown in Fig. 7. As shown in Fig. 8. At around 70% stress, HPC began to fracture. At roughly 85% stress, more cracks started to appear on faces. Eventually, at roughly 95% stress, the corners collapsed. The same cracking occurred in smaller specimens (100 mm × 100 mm × 100 mm), but the first cracking was produced at a greater stress level roughly 75% which increased the concrete's compressive strength. In the end, the cubes break, as shown in Fig. 8.

A brief visual inspection shows that the cubes damaged more than the cylinders. As illustrated in Figs. 9 and 10. cylinders formation a first inclined fracture surface, The Fig. 8 demonstrates ultimate cracking pattern of cubes. All cylinders subsequently separated together to form a diagonal fracture plane, as shown in Figs. 9 and 10. The initial crack in HPC cylinders was seen to occur at approximately 85 percent of ultimate stress in the current investigation, and additional loading propagates the same crack, getting started the failure with fewer cracks.

The determination of the initial crack in material testing involves subjecting specimens to gradual loading while monitoring their response. Stress levels are gradually increased, and crack initiation is detected through methods like visual inspection. The process aims to identify the stress level at which the first crack appears, often expressed as a percentage of the material's ultimate strength. This information is crucial for assessing the material's fatigue behavior and fracture mechanics. The 85% stress level mentioned may be a specific threshold defined by testing standards or protocols.

The aspects related to the evaluation of concrete properties, specifically focusing on the shape and size effects in accordance with EN 206 standards. Comparisons can be made using cubes, particularly referring to the second parts of

**Table 9** Mechanical properties of high-performance concrete

| Grade of concrete in MPa | Cube strength $f_{cu}$ in N/mm$^2$ | Cylindrical strength $f_c'$ in N/mm$^2$ | Elastic modulus $E_c$ in GPa |
|---|---|---|---|
| 60 | 75.83 | 62.00 | 40.40 |
| 60 | 73.86 | 70.90 | 41.84 |
| 60 | 76.51 | 68.00 | 40.20 |
| 60 | 74.10 | 65.00 | 40.43 |
| 60 | 77.63 | 66.71 | 38.18 |
| 70 | 78.83 | 67.00 | 42.40 |
| 70 | 80.86 | 70.90 | 44.84 |
| 70 | 79.51 | 68.00 | 42.20 |
| 70 | 80.10 | 67.00 | 44.43 |
| 70 | 78.63 | 70.71 | 43.18 |
| 80 | 83.85 | 77.58 | 45.42 |
| 80 | 93.65 | 88.00 | 45.05 |
| 80 | 82.35 | 74.36 | 45.47 |
| 80 | 88.89 | 78.00 | 44.61 |
| 80 | 90.87 | 82.00 | 45.27 |



**Fig. 6** Coalescence of cracks near the corners



**Fig. 7** Vertical Cracks leading to Column fragments

**Fig. 8** Ultimate Cracking pattern of Cubes



**Fig. 9** Nucleation of inclined fracture surface and diagonal fracture zone
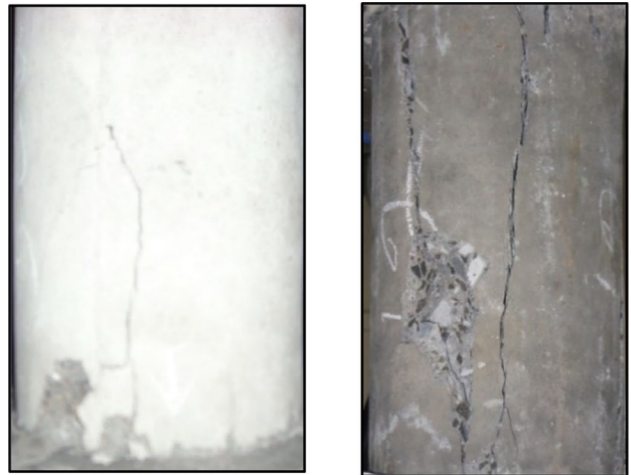


**Fig. 10** Ultimate Cracking pattern of cylinders

the C60/75, C70/85, C80/95 classifications specified in EN 206 standards. For C60/75, a comparison is made based on achieving a compressive strength of 75 MPa. If the concrete achieves 75 MPa, it is categorized under the C60 class. The standard size of cube samples used is 15 cm × 15 cm × 15cm. The size effect is noted as being effective, indicating that the size of the concrete samples has an impact on the properties being evaluated.

### 5.3 Tensile strength of concrete

Concrete has a comparatively high compression strength but a low-tension strength. Because reinforcement is given to resist all tensile stresses, reinforced concrete members place not much value on the tensile strength of concrete. Tensile stresses within concrete exhibit heightened sensitivity to various factors such as drying shrinkage, corrosion of reinforcement, temperature discrepancies, and a range of other variables. Consequently, possessing a comprehensive understanding of concrete's tensile strength assumes paramount importance. The assessment of concrete's tensile strength is conducted through two prescribed tests outlined as follows:

1. Split Tensile Strength Test.
2. Flexure Strength Test.

#### 5.3.1 Split tensile strength

It is also referred to as the indirect tension test method. The "Brazilian Test" is another name for this. In 1943, Brazil created this test. This was separately created in Japan around the same time. This test is performed by inserting a cylindrical specimen horizontally between the loading surfaces of compression testing equipment and applying a load along its vertical length until the cylinder fails.

The key benefit of this procedure is that it may utilise the same specimen and testing apparatus as the compression test. As a result, this type of examination is becoming increasingly common. The split tensile strength test is characterized by its relative simplicity in execution and its capacity to generate results of greater precision compared to alternative tension testing methods. The configuration of the cylinder subjected to the split tensile strength test is illustrated in Fig. 11. Notably, the split tensile strength is acknowledged for its closer alignment with concrete's authentic tensile strength in contrast to the modulus of rupture.

As illustrated in Fig. 11, an empirical relationship for split tensile strength has been established.

$$f_{t1} = 0.565\sqrt{f_c'} in MPa \tag{5.1}$$

$$f_{t2} = 0.536\sqrt{f_{cu}} in MPa \tag{5.2}$$

The comparison between Eq. 5.1 and the analytical equations provided by [5, 6, 12, 22, 24, 28] can be seen in Fig. 14. The calculation approach proposed by [28] is limited to concrete strengths of up to 80 MPa. The suggested equation in

**Fig. 11** Cylinder tested for split tension test
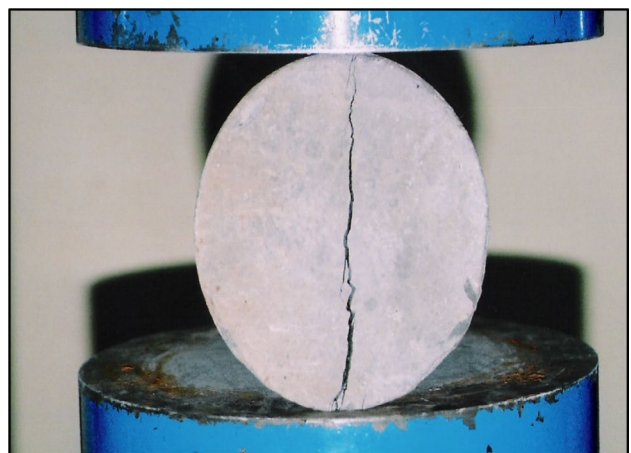
**Fig. 12** Relation between cylindrical strength and split tensile strength of HPC
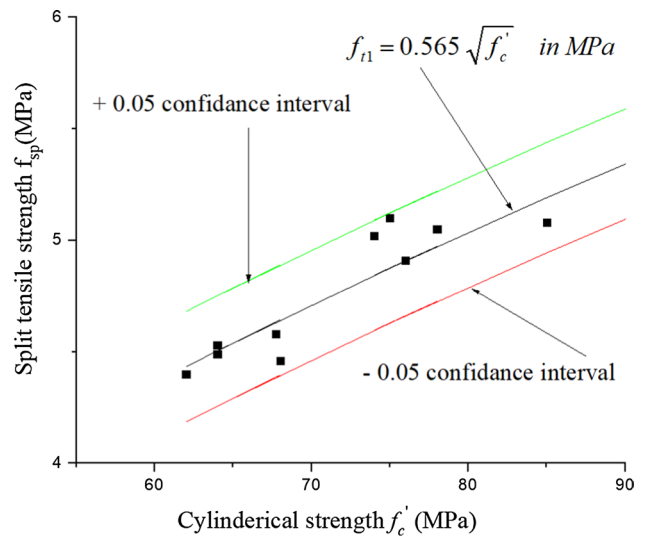


$$f_{t1} = 0.565 \sqrt{f_c'} \quad in \; MPa$$

+ 0.05 confidance interval

- 0.05 confidance interval

**Fig.13** Relation between cylindrical strength of concrete and split tensile strength and error bars to indicate spread of data



Standard Deviation = 0.55 N/mm$^2$
Average          = 5.22 N/mm$^2$

Spread of Data of erros for Split strength of concrete

**Fig. 14** Comparison of analytical equations for split tensile strength



Present study

- ACI-318-08
- ACI363R
- Ahmed and Shah
- S. Bhanja and B. Sengupta
- Irvani Said
- Selim Pul
- Present study
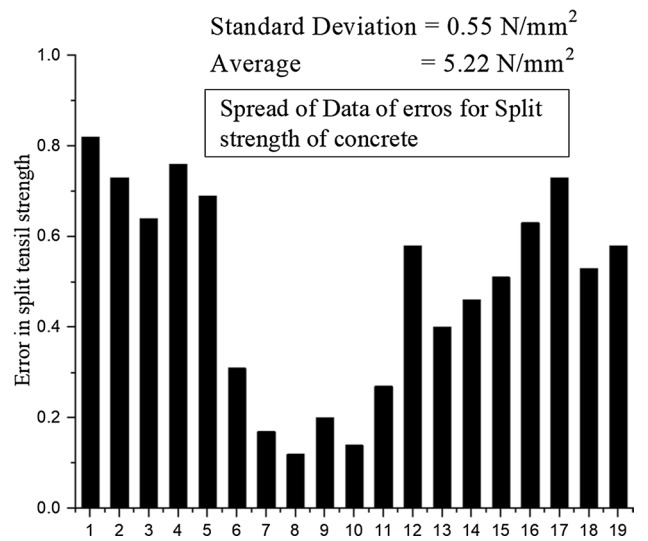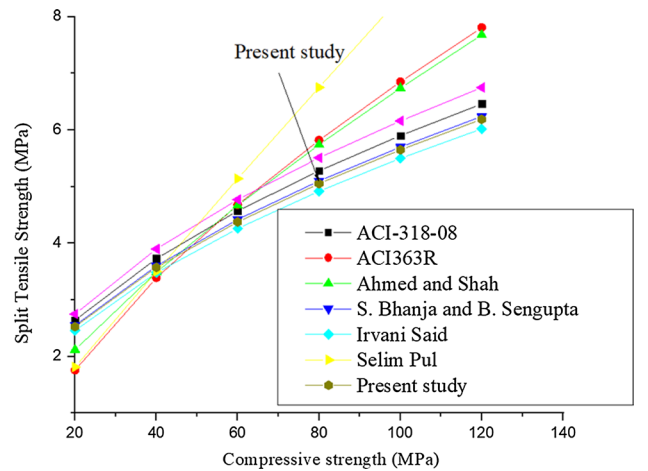
**Fig. 15** Modulus of rupture test with flexure crack near the centre of beam



**Fig. 16** Relation between cylindrical strength Flexural tensile strength of HPC
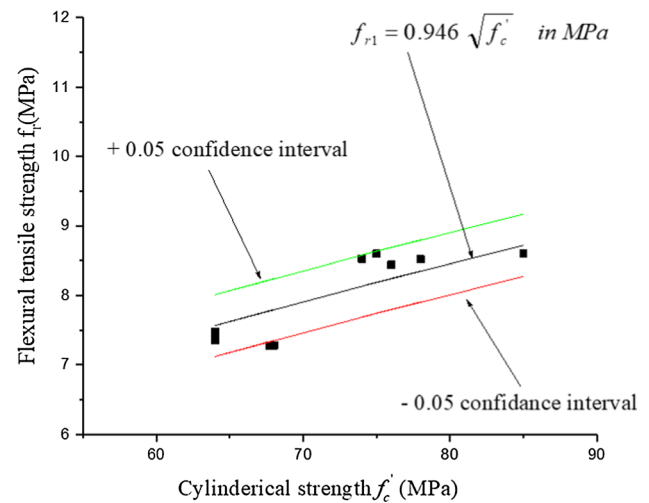


this study is in very close agreement with those of [4, 22, 24] and it matches that of [12]. Nevertheless, the formulas [5, 6, 28] overstate the split tensile strength. The Relation between cylindrical strength and split tensile strength of HPC is as shown in the Fig. 12.

The Relation between cylindrical strength of concrete and split tensile strength and error bars to indicate spread of data is as shown in Fig. 13. For preparation of High-Performance Concrete (HPC), the American Concrete Institute [4] gives specialized guidelines, provide a good approach to address the unique challenges of HPC, ensuring optimal mix design, durability, and performance. Its emphasis on quality assurance, support for innovation and research. The Comparison of analytical equations for split tensile strength is shown in Fig. 14.

### 5.3.2 Modulus of rupture

The modulus of rupture (extreme fibre stress in bending) is affected by beam size and loading technique. The middle point loading and third-point loading are the loading processes used to determine flexure tension. Below the loading point with the greatest bending moment, the maximum fibre stress will occur. When dealing with symmetrical two-point loading scenarios, a critical fracture could arise at any point lacking the requisite strength to withstand the stress within the central third of the structure. It is to be expected that two-point loading would yield a modulus of rupture value lower than that observed in central point loading. This testing configuration is visually depicted in Fig. 15, in accordance with the guidelines outlined in IS 516-1959.

Figure 16 and Fig. 17 show the flexural tensile strength results. The flexural strength relationships are obtained by using regression analysis, as illustrated below.

**Fig. 17** Relation between compressive strength of concrete and flexure tensile strength and error bars to indicate spread of data
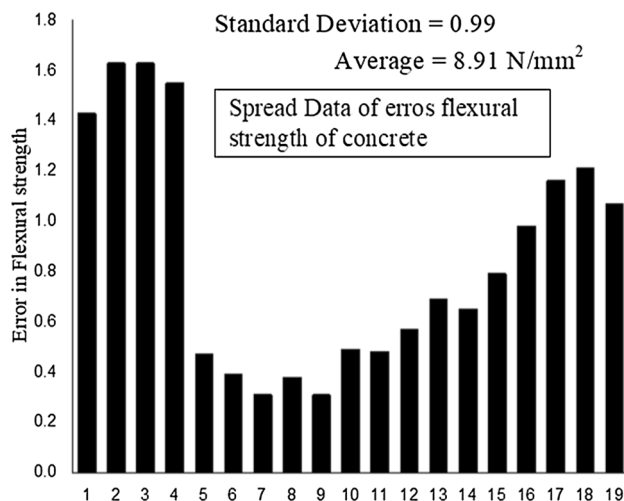


$$f_{r1} = 0.946\sqrt{f'_c}\, inMPa \tag{5.3}$$

$$f_{r2} = 0.90\sqrt{f_{cu}}\, inMPa \tag{5.4}$$

With the use of the analytical equations provided by [12, 16, 22, 24, 28] the current data is compared to Eq. 5.3, as seen in Fig. 18. The equation proposed by [22] and the current study are comparable, and both totally comply with ACI 363. The equations of [2, 16] overestimate the modulus of rupture. The equation by [12] overestimates at high strength levels and underestimates flexure tensile strength at low strength levels. There is not a single equation in the literature that agrees with [28] formula.

## 5.4 Modulus of elasticity of concrete

As shown in Fig. 19a–d, stress–strain curves have been generated for various concrete strengths. Elasticity moduli are assessed at 40% stress level and are shown in Table 10. Regression analysis of the current study's data shows the following relationship for Ec.

$$E_{c1} = 5050\sqrt{f'_c}\, inMPa \tag{5.5}$$

**Fig. 18** Comparison of analytical equations for flexure tensile strength

a Stress-strain curves of 60 MPa concrete



b Stress -strain curves of 70 MPa concrete



c Stress -strain curves of 80 MPa concrete



d Stress-strain (Longitudinal and lateral) curve for 60 MPa to 80 MPa
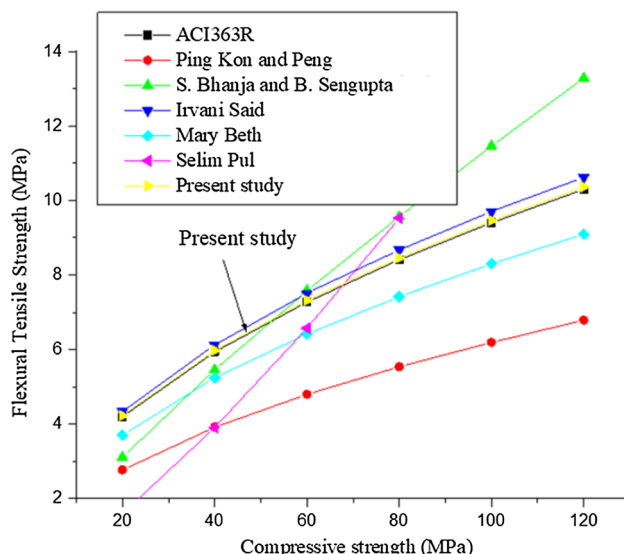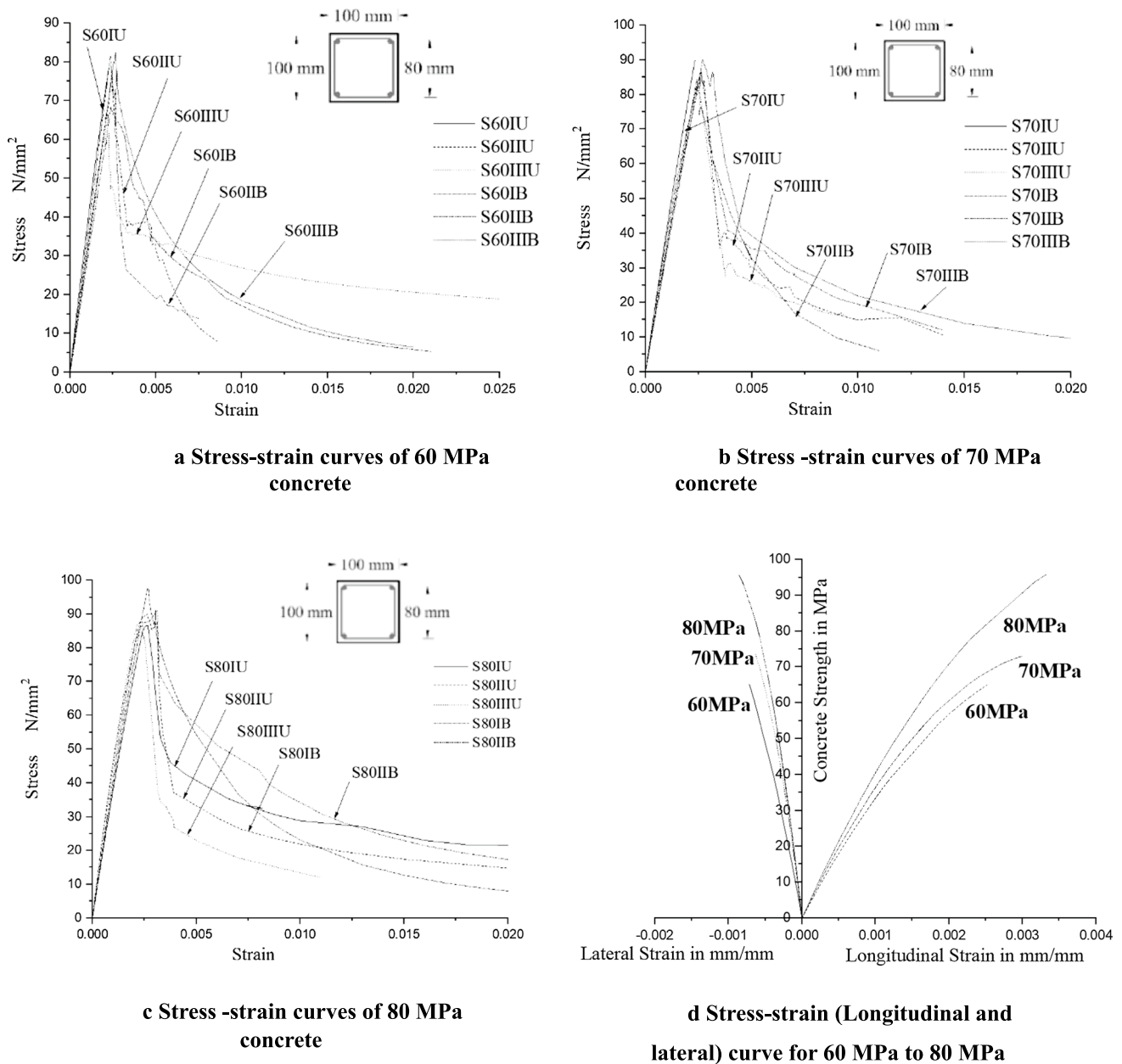
Fig.19  (a–d) Stress–strain relationships in uni-axial compression

$$E_{c2} = 4800\sqrt{f_{cu}}\, in\, MPa \qquad (5.6)$$

Figure 20 provides a visual representation of the relationship between each specimen's elastic modulus (Ec) and the concrete strength (fc'). Several attempts have been made to establish a link between the modulus of elasticity and concrete strength because of the significant impact that the former has on the other. Figure 21 shows 211 data points from the literature. 39 specimens from [35] data (40–125 MPa), 48 specimens from [21] data (60–100 MPa), 37 specimens from [27] data (14–47 MPa), 36 specimens from [34] data (20–30 MPa), 25 specimens [22] data (60–120 MPa).

In the context of stress–strain graphs for High-Performance Concrete (HPC) mixes with designations M60, M70, and M80, an increase in strength without a corresponding decrease in deformation might appear counterintuitive. Generally, as concrete strength increases, it is expected that ductility and deformability decrease, leading to a potentially brittle behavior. However, the apparent increase in toughness without additional contributions such as

**Table 10** Experimental Values of modulus of elasticity and Poisson's ratio

| Grade of concrete in MPa | Cube Strength $f_{cu}$ in N/mm$^2$ | Cylindrical Strength $f_c'$ in N/mm$^2$ | Elastic Modulus $E_c$ in GPa | Peak/Ultimate Strain in mm/mm | Poisson's ratio |
|---|---|---|---|---|---|
| 60 | 75.83 | 62.00 | 40.40 | 0.0023 | 0.187 |
| 60 | 73.86 | 70.90 | 41.84 | 0.0028 | 0.198 |
| 60 | 76.51 | 68.00 | 40.20 | 0.0027 | 0.159 |
| 60 | 74.10 | 65.00 | 40.43 | 0.0026 | 0.146 |
| 60 | 77.63 | 74.71 | 38.18 | 0.0024 | 0.185 |
| 70 | 78.85 | 75.58 | 42.42 | 0.0025 | 0.155 |
| 70 | 79.65 | 74.00 | 42.05 | 0.0026 | 0.154 |
| 70 | 79.35 | 74.36 | 43.47 | 0.0026 | 0.162 |
| 70 | 80.89 | 75.00 | 43.61 | 0.0027 | 0.167 |
| 70 | 80.87 | 73.00 | 43.97 | 0.0027 | 0.165 |
| 80 | 83.85 | 77.58 | 45.42 | 0.0030 | 0.135 |
| 80 | 93.65 | 88.00 | 45.05 | 0.0026 | 0.154 |
| 80 | 82.35 | 74.36 | 45.47 | 0.0027 | 0.182 |
| 80 | 88.89 | 78.00 | 44.61 | 0.0030 | 0.196 |
| 80 | 90.87 | 82.00 | 45.27 | 0.0029 | 0.165 |

**Fig.20** Values of elastic modulus of present research and others in the literature
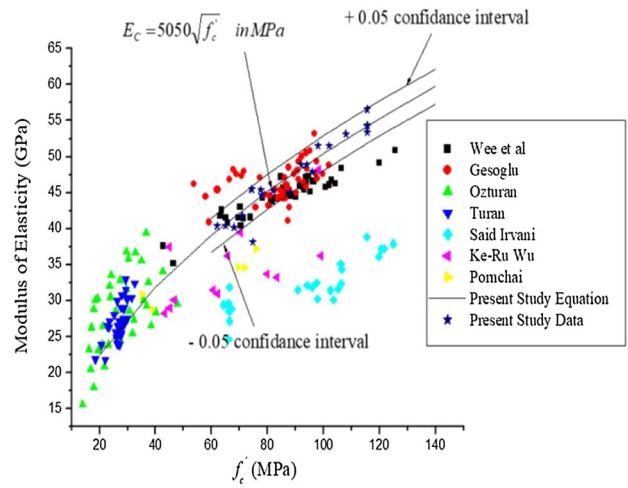


**Fig.21** Error bars to indicate the spread of data
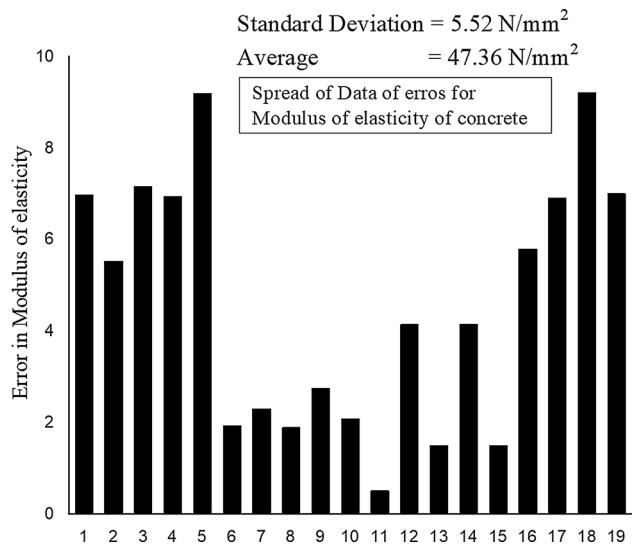
**Table 11** Equations for modulus of elasticity by codes and researchers

| Sr. No | Researchers Name/ Code | Equation suggested |
|---|---|---|
| 01 | Euro Code 2 | $E_c = 21500\left[\frac{f_c'}{10}\right]^{\frac{1}{3}}$ |
| 02 | Gardener | $E_c = 3500 + 4300\sqrt{f_c'}$ |
| 03 | ACI 363 | $E_c = 6900 + 3300\sqrt{f_c'}$ 21 MPa $< f_c' <$ 83 MPa |
| 04 | CSA 23.3–94 | $E_c = 5050\sqrt{f_c'}$ |
| 05 | Mary Beth | $E_c = 5230\sqrt{f_c'}$ 40 MPa $< f_c' <$ 90 MPa |
| 06 | IS 456–2000 | $f_{t2} = 0.536\sqrt{f_{cu}}$ in MPa $f_{ck}$ is characteristic strength of concrete |



**Fig. 22** Values of Poisson's ratio of the present study and other researchers
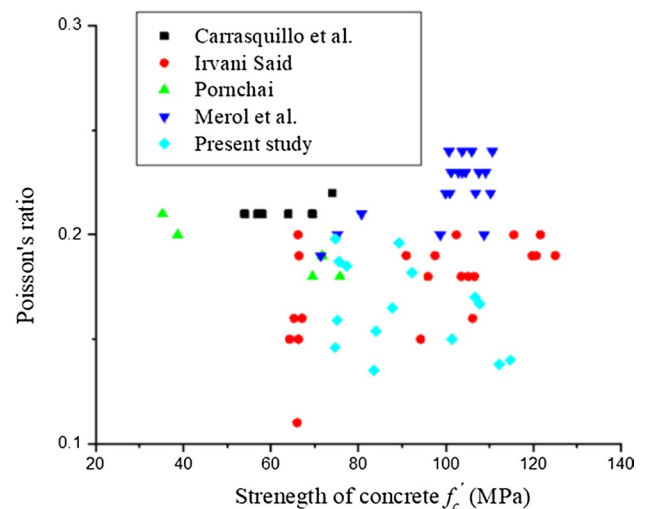
fibre reinforcement could be attributed to several factors. The concrete mix design, the presence of supplementary cementitious materials such as silica fume, and any unique additives could influence the overall mechanical behavior. Additionally, advancements in concrete technology, including the use of optimized particle gradations and chemical admixtures, can enhance both strength and deformability. To comprehensively interpret the observed stress–strain behaviour, a detailed analysis of the specific mix proportions, materials used, and any reinforcing mechanisms is essential. Table 10 shows the Experimental Values of modulus of elasticity and Poisson's ratio.

Ec values obtained in the present study range from 40 and 50 GPa. Table 11 shows some of the equations given for Ec by codes and researchers. When compared to other equations, the current study equation perfectly matches that proposed in CSA 23.3–94. IS 456–2000's equations overestimate the modulus of elasticity.

## 5.5 Poisson's ratio

The cubes were tested to determine Poisson's ratios. Micro cracking begins to develop parallel to the direction of stress at higher stress levels. Transverse strain increases as the stress increases. Poisson's ratio rapidly increases near maximum strength until failure occurs. As a result, at 40% axial stress, the Poisson's ratio is determined, which corresponds to the point at which the elastic modulus is estimated. Table 11 displays the results of the current investigation. The non-evaluation of Poisson's ratio for 80 MPa concrete is attributed to the challenges arising from the intricacies of instrumenting specimens sized at 100 mm × 100 mm × 100 mm. Additionally, the constrained availability of pi-gauges featuring a gauge length of 50 mm further contributes to the unaddressed status of this parameter. For concrete strengths of 60 MPa, 70 MPa, and 80 MPa, the Poisson's ratio average values are 0.175, 0.166, and 0.153, respectively. Figure 22 shows the findings of this study as well as those of other investigators, including [15, 22] Mertol et al. 2016. While a definitive trend for Poisson's ratio may not be

apparent, the findings of the present study suggest that an enhancement in concrete strength correlates with a reduction in the average value of Poisson's ratio.

## 5.6 Testing of columns
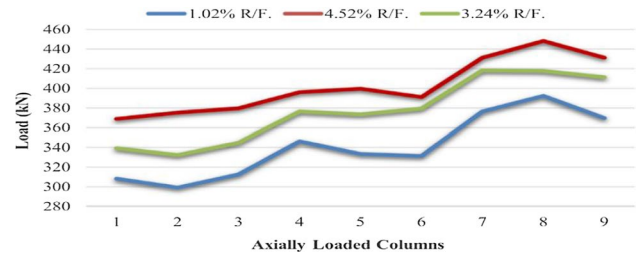
### 5.6.1 Columns under axial compression

Twenty-seven columns were tested, with concrete strengths ranging up to 80Mpa. The columns were subjected to axial loads using a 1000 kN capacity loading frame, with load cells and a data acquisition system used to measure the applied load. The maximum deflection observed for the 60 MPa concrete was 0.98 mm, for the 70 MPa concrete it was 0.63 mm, and for the M80 concrete, it was 0.61 mm at the ultimate load of 394.37 kN. Similarly, all deflection for all columns noted at midspan. Table 12 presents the maximum load and deflection recorded for the axially loaded columns.

The average strength of M60 concrete exhibited an increase of 10.43% and 22.03% when the reinforcement percentages were 3.14% and 4.52%, respectively, compared to the reference reinforcement percentage of 2.01%. Similarly, the strength of M70 concrete showed an increase of 11.67% and 17.31%, while the strength of M80 concrete demonstrated an increase of 9.48% and 15.01%. The variation in load for axially loaded columns with different longitudinal reinforcement percentages is illustrated in Fig. 23.

| Table 12 Test outcomes of axially loaded square specimens | Grade of HPC | Reinforcement Percentage (%) | Column Designation | $f_{cu}$ MPa | $f'_c$ MPa | $P_{max}$ kN | Max. Deflection mm |
|---|---|---|---|---|---|---|---|
| | M60 | 2.01 | SC60IA1 | 67.98 | 54.26 | 310.16 | 0.95 |
| | | | SC60IA2 | 67.08 | 55.19 | 301.28 | 0.92 |
| | | | SC60IA3 | 67.9 | 55.73 | 314.61 | 0.98 |
| | | 3.24 | SC60IIA1 | 66.04 | 53.96 | 341.28 | 0.86 |
| | | | SC60IIA2 | 67.31 | 55.18 | 334.41 | 0.87 |
| | | | SC60IIA3 | 66.6 | 54.66 | 346.94 | 0.91 |
| | | 4.52 | SC60IIIA1 | 68.51 | 55.08 | 371.01 | 0.77 |
| | | | SC60IIIA2 | 67.1 | 53.48 | 377.2 | 0.82 |
| | | | SC60IIIA3 | 65.92 | 52.46 | 381.84 | 0.85 |
| | M70 | 2.01 | SC70IA1 | 76.24 | 62.37 | 348.28 | 0.61 |
| | | | SC70IA2 | 78.05 | 63.57 | 335.37 | 0.63 |
| | | | SC70IA3 | 73.25 | 61.78 | 333.3 | 0.55 |
| | | 3.24 | SC70IIA1 | 74.02 | 62.18 | 378.58 | 0.5 |
| | | | SC70IIA2 | 73.33 | 61.54 | 375.48 | 0.53 |
| | | | SC70IIA3 | 74.42 | 63.45 | 381.57 | 0.51 |
| | | 4.52 | SC70IIIA1 | 76.38 | 62.22 | 398.15 | 0.4 |
| | | | SC70IIIA2 | 77 | 64.09 | 401.57 | 0.42 |
| | | | SC70IIIA3 | 72.1 | 65.14 | 393.26 | 0.38 |
| | M80 | 2.01 | SC80IA1 | 85.98 | 69.96 | 378.59 | 0.53 |
| | | | SC80IA2 | 85.19 | 68.56 | 394.37 | 0.61 |
| | | | SC80IA3 | 86.61 | 69.78 | 371.89 | 0.45 |
| | | 3.24 | SC80IIA1 | 85.08 | 66.14 | 420.37 | 0.4 |
| | | | SC80IIA2 | 84.1 | 68.53 | 419.68 | 0.43 |
| | | | SC80IIA3 | 82.03 | 67.71 | 413.37 | 0.37 |
| | | 4.52 | SC80IIIA1 | 86.24 | 65.07 | 433.15 | 0.28 |
| | | | SC80IIIA2 | 85.1 | 67.14 | 450.26 | 0.31 |
| | | | SC80IIIA3 | 84.11 | 66.25 | 433.26 | 0.25 |

**Fig. 23** Load Variation for Axially loaded columns



## 5.6.2 Columns under uni-axial compression

A total of 27 concrete column specimens with strengths ranging from 60 to 80 MPa were subjected to uniaxial loading with an eccentricity of 20% (20 mm) from the longer face. The recorded maximum deflections for different concrete strengths were as follows: 1.27 mm for 60 MPa, 1.03 mm for 70 MPa, and 0.96 mm for 80 MPa at a maximum load of 361.02kN.

One long column, constructed using M60 concrete with a reinforcement percentage of 2.01%, sustained an average load of 288.95kN, resulting in an average deflection of 1.22 mm. For reinforcement percentages of 3.14% and 4.52%, the average loads were 317.59kN and 344.34kN, respectively, with corresponding average deflections of 1.14 mm and 0.94 mm. Similarly, remaining columns shows good relation for midspan deflection with respect to load. Table 13 summarizes the maximum load and deflection recorded for the uniaxially loaded columns.

**Table 13** Test outcomes of Uniaxially loaded square specimens

| Grade of HPC | Reinforcement Percentage (%) | Column Designation | $f_{cu}$ MPa | $f'_c$ MPa | $P_{max}$ kN | Max. Deflection mm |
|---|---|---|---|---|---|---|
| M60 | 2.01 | SC60IU1 | 68.28 | 55.27 | 284.43 | 1.23 |
| | | SC60IU2 | 65.43 | 52.2 | 297.66 | 1.24 |
| | | SC60IU3 | 67.65 | 53.84 | 284.76 | 1.18 |
| | 3.24 | SC60IIU1 | 67.92 | 53.97 | 314.19 | 1.17 |
| | | SC60IIU2 | 66.43 | 52.49 | 325.32 | 1.13 |
| | | SC60IIU3 | 65.84 | 53.67 | 313.25 | 1.11 |
| | 4.52 | SC60IIIU1 | 69.11 | 55.39 | 343.22 | 0.89 |
| | | SC60IIIU2 | 64.97 | 51.89 | 355.09 | 0.98 |
| | | SC60IIIU3 | 66.81 | 53.77 | 334.71 | 0.95 |
| M70 | 2.01 | SC70IU1 | 74.33 | 59.98 | 323 | 1.01 |
| | | SC70IU2 | 75.85 | 60.98 | 305.35 | 0.9 |
| | | SC70IU3 | 76.25 | 61.82 | 313.76 | 0.94 |
| | 3.24 | SC70IIU1 | 78.32 | 63.72 | 349.17 | 0.89 |
| | | SC70IIU2 | 74.83 | 60.75 | 348.46 | 0.96 |
| | | SC70IIU3 | 76.22 | 62.19 | 336.98 | 0.89 |
| | 4.52 | SC70IIIU1 | 77.71 | 62.87 | 378.08 | 0.85 |
| | | SC70IIIU2 | 79.6 | 65.6 | 367.09 | 0.75 |
| | | SC70IIIU3 | 78.7 | 64.75 | 363.95 | 0.73 |
| M80 | 2.01 | SC80IU1 | 85.38 | 68.92 | 354.36 | 0.85 |
| | | SC80IU2 | 83.89 | 67.57 | 363.76 | 0.97 |
| | | SC80IU3 | 86.71 | 69.79 | 355.79 | 0.93 |
| | 3.24 | SC80IIU1 | 87.08 | 70.15 | 394.55 | 0.74 |
| | | SC80IIU2 | 85.7 | 67.84 | 392.43 | 0.71 |
| | | SC80IIU3 | 83.77 | 65.89 | 391.36 | 0.8 |
| | 4.52 | SC80IIIU1 | 86.8 | 65.39 | 410.7 | 0.52 |
| | | SC80IIIU2 | 84.55 | 68.75 | 417.66 | 0.57 |
| | | SC80IIIU3 | 86.11 | 64.76 | 424.89 | 0.63 |

**Fig. 24** Load Variation for Uniaxially loaded columns
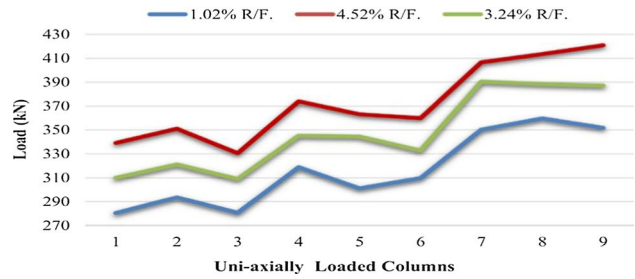


When compared to the reference reinforcement percentage of 2.01%, the average deflection of M60 concrete demonstrated an increase of 7.04% and 29.43% for reinforcement percentages of 3.14% and 4.52%, respectively. Similarly, the strength of M70 concrete showed an increase of 4.01% and 22.32%, while the strength of M80 concrete exhibited an increase of 22.22% and 59.88%.

Figure 24 shown below depicts the variation in load for the uniaxially loaded columns with different longitudinal reinforcement percentages. In comparison to a reinforcement percentage of 2.01%, the average strength of M60 concrete exhibited an increase of 9.9% and 19.17% for reinforcement percentages of 3.14% and 4.52%, respectively. Similarly, the strength of M70 concrete was observed to increase by 9.82% and 17.73%, while the strength of M80 concrete demonstrated an increase of 9.72% and 16.70%.

**Table 14** Test outcomes of Biaxially loaded square specimens

| Grade of HPC | Reinforcement Percentage (%) | Column Designation | $f_{cu}$ MPa | $f'_c$ MPa | $P_{max}$ kN | Max. Deflection mm |
|---|---|---|---|---|---|---|
| M60 | 2.01 | SC60IB1 | 64.02 | 52.04 | 265.19 | 3.01 |
| | | SC60IB2 | 66.01 | 52.97 | 269.40 | 3.09 |
| | | SC60IB3 | 65.1 | 51.62 | 261.81 | 2.97 |
| | 3.24 | SC60IIB1 | 62.92 | 54.24 | 290.59 | 2.96 |
| | | SC60IIB2 | 68.41 | 55.5 | 296.7 | 2.93 |
| | | SC60IIB3 | 66.92 | 53.31 | 293.52 | 2.95 |
| | 4.52 | SC60IIIB1 | 65.16 | 52.73 | 312.89 | 2.71 |
| | | SC60IIIB2 | 63.96 | 54.43 | 319.74 | 2.68 |
| | | SC60IIIB3 | 66.74 | 52.3 | 323.5 | 2.75 |
| M70 | 2.01 | SC70IB1 | 73.14 | 65.34 | 297.98 | 2.99 |
| | | SC70IB2 | 75.40 | 61.85 | 281.83 | 2.9 |
| | | SC70IUB3 | 77.22 | 64.57 | 289.36 | 2.93 |
| | 3.24 | SC70IIB1 | 73.18 | 63.01 | 312.58 | 2.65 |
| | | SC70IIB2 | 74.39 | 62.81 | 320.92 | 2.68 |
| | | SC70IIB3 | 76.22 | 61.57 | 310.68 | 2.66 |
| | 4.52 | SC70IIIB1 | 73.99 | 64.69 | 339.54 | 2.53 |
| | | SC70IIIB2 | 71.98 | 65.37 | 351.68 | 2.58 |
| | | SC70IIIB3 | 71.77 | 62.29 | 352.19 | 2.53 |
| M80 | 2.01 | SC80IB1 | 83.41 | 68.24 | 314.41 | 2.76 |
| | | SC80IB2 | 82.19 | 67.24 | 319.18 | 2.82 |
| | | SC80IB3 | 84.07 | 69.8 | 329.69 | 2.87 |
| | 3.24 | SC80IIB1 | 83.56 | 66.64 | 358.52 | 2.35 |
| | | SC80IIB2 | 82.44 | 67.28 | 369.24 | 2.38 |
| | | SC80IIB3 | 84.05 | 69.81 | 357.71 | 2.36 |
| | 4.52 | SC80IIIB1 | 85.4 | 70.25 | 375.37 | 1.95 |
| | | SC80IIIB2 | 83.23 | 66.93 | 386.66 | 2.12 |
| | | SC80IIIB3 | 86.19 | 68.67 | 382.58 | 1.98 |

**Fig. 25** Load Variation for Bi-axially loaded columns
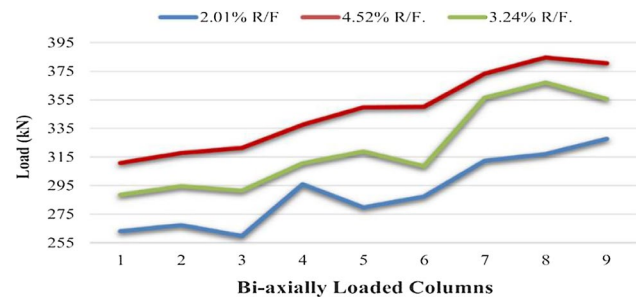


### 5.6.3 Columns under Bi-axial compression

A total of twenty-seven column specimens with concrete strengths ranging from 60 to 80 MPa were subjected to biaxial loading, with a 20% eccentricity about both axes, resulting in a diagonal eccentricity of 28.28 mm. The testing was conducted using a loading frame with a capacity of 1000 kN. The maximum deflections recorded for different concrete strengths were as follows: 3.02 mm for 60 MPa, 2.95 mm for 70 MPa, and 2.71 mm for 80 MPa at an ultimate load of 312.89 kN. The biaxially loaded column shows a maximum defection at midspan as compare to uniaxial lading. Table 14 presents the maximum load and deflection recorded for the biaxial column.

In comparison to a reinforcement percentage of 2.01%, the average deflection of M60 concrete was found to increase by 2.60% and 11.43% for reinforcement percentages of 3.14% and 4.52%, respectively. Similarly, the strength of M70 concrete was observed to increase by 10.39% and 15.45%, while the strength of M80 concrete exhibited an increase of 19.18% and 39.67%. Figure 25 illustrates the variation in load for the bi-axially loaded columns with different longitudinal reinforcement percentages.

In comparison to a reinforcement percentage of 2.01%, the average strength of M60 concrete was found to increase by 10.60% and 20.06% for reinforcement percentages of 3.14% and 4.52%, respectively. Similarly, the strength of M70 concrete was observed to increase by 8.63% and 20.05%, while the strength of M80 concrete exhibited an increase of 12.68% and 18.82%.

## 6 Conclusion

1. High-performance concrete's (HPC) essential mechanical properties, including modulus of elasticity, split tensile strength, flexure tensile strength, and compressive strength, were examined in this particular study. Based on their experimental findings, the researchers additionally proposed mathematical models for these features.
2. The mechanical properties of concrete can be considerably enhanced by the researchers through the use of novel components and optimised mix proportions. Compared to regular concrete, HPC has superior durability, flexural strength, and compressive strength. This improves the structure's ability to support large loads and resist off deterioration over time.
3. Concrete's mechanical properties may be enhanced and the environmental effect of concrete manufacture can be decreased by adding various cementitious materials, such as fly ash, slag and silica fume.
4. The use of mineral admixtures like fly ash and silica fume in HPC positively influences its mechanical properties by enhancing strength, improving durability and reducing the permeability.
5. The suggested mix design method is efficient in producing high-performance concrete (HPC) with the required strength, offering both effectiveness and cost-effectiveness, while also being easy to implement.
6. The concrete's split tensile strength and flexural strength are directly related to its compressive strength, which is in line with ACI guidelines and Iravani Said formulae. These relationships hold true for strengths up to 120 MPa.
7. The average Poisson's ratio is 0.165, falling within the generally accepted range of 0.15 to 0.25.
8. The researchers proposed keeping the ultimate concrete strain constant at 0.003, in line with the ACI 318 (2008) code. They also proposed a capacity reduction factor for columns in concentric compression and stress-block parameters for HPC. They found that the proposed parameters are conservative.
9. The split tensile strength, flexural strength, and modulus of elasticity of concrete are correlated with its compressive strength. They also agree well with many formulas proposed in the existing literature.

10. The average Poisson's ratio obtained for concrete strengths ranging from 60 to 80 MPa is 0.165.
11. For bi-axially loaded columns, the M60 grade concrete with 2.01% longitudinal reinforcement exhibits higher midspan deflections compared to M70 and M80 grade concrete. Conversely, the M80 grade concrete with 4.52% longitudinal reinforcement demonstrates greater load-carrying capacity compared to the other grades.

## Declarations

## References

1. Abdal S, Mansour W, Agwa I, Nasr M, Abadel A, Onuralp Özkılıç Y, Akeed MH. Application of ultra-high-performance concrete in bridge engineering: current status, limitations, challenges, and future prospects. Buildings. 2023;13(1):185. https://doi.org/10.3390/buildings13010185.
2. Abdal S, Siddique I, Afzal S, Chu YM, Ahmadian A, Salahshour S. On development of heat transportation through bioconvection of Maxwell nanofluid flow due to an extendable sheet with radiative heat flux and prescribed surface temperature and prescribed heat flux conditions. Math Methods Appl Sci. 2023;46(10):11355–72.
3. Aboukifa M, Moustafa MA. Structural and buckling behavior of full-scale slender UHPC columns. Eng Struct. 2022;255: 113928. https://doi.org/10.1016/j.engstruct.2022.113928.
4. ACI 318 R-02, Building Code Requirements for Structural Concrete (ACI 318-02) and Commentary (ACI 318R-02), American Concrete Institute.
5. ACI 363: High-Strength Concrete (ACI 363R)
6. Ahmad SH, Shah SP, ACI J 1982;79-6:484-490
7. Ahmad SH, Shah SP. Structural properties of high strength concrete and its implications for precast prestressed concrete. PCI J. 1985;30(6):92–119.
8. Aitcin PC. High-performance Concrete (E & FN Spon. An imprint of Routledge 11 New Fetter Lane, London), 1998.
9. Akeed MH, Qaidi S, Ahmed HU, Faraj RH, Mohammed AS, Emad W, Azevedo AR. Ultra-high-performance fiber-reinforced concrete. Part IV: Durability properties, cost assessment, applications, and challenges. Case Stud Construct Mater. 2022;17: e01271. https://doi.org/10.1016/j.cscm.2022.e01271.
10. Amran M, Fediuk R, Abdelgader HS, Murali G, Ozbakkaloglu T, Lee YH, Lee YY. Fiber-reinforced alkali-activated concrete: a review. J Build Eng. 2022;45: 103638.
11. Amran M, Huang SS, Onaizi AM, Makul N, Abdelgader HS, Ozbakkaloglu T. Recent trends in ultra-high performance concrete (UHPC): current status, challenges, and future prospects. Constr Build Mater. 2022;352: 129029. https://doi.org/10.1016/j.conbuildmat.2022.129029.
12. Bhanja S, Sengupta B. Investigations on the tensile strength of high performance concrete incorporating silica fume. 2005
13. Bliuc R. Particularities of the structural behaviour of reinforced high strength concrete slabs (Doctoral dissertation, UNSW Sydney). 2004.
14. Byrne G, Ahearne E, Cotterell M, Mullany B, et al. High performance cutting (HPC) in the new era of digital manufacturing–a roadmap. Procedia Cirp. 2016;46:1–6. https://doi.org/10.1016/j.procir.2016.05.038.
15. Carrasquillo RL, Nilson AH, Slte FO, ACI J 1981;78-3:171-178.
16. Ping-Kun C, Yaw-Nan P, Cem Concr Res 2001;31:87-95
17. De Brito J, Ferreira J, Pacheco J, Soares D, Guerreiro M. Structural, material, mechanical and durability properties and behaviour of recycled aggregates concrete. J Build Eng. 2016;6:1–16.
18. Elyasigorji F. Reactivity assessment of pozzolanic materials for partial replacement of cement in concrete. 2023.

19. Farhangi V, Moradi MJ, Daneshvar K, Hajiloo H. Application of artificial intelligence in predicting the residual mechanical properties of fiber reinforced concrete (FRC) after high temperatures. Constr Build Mater. 2024;411: 134609.

20. Gencel O, Brostow W, Datashvili T, Thedford M. Workability and mechanical performance of steel fiber-reinforced self-compacting concrete with fly ash. Compos Interfaces. 2011;18(2):169–84. https://doi.org/10.1163/092764411X567567.

21. Gesoglu M, Güneyisi E, Asaad DS, Muhyaddin GF. Properties of low binder ultra-high performance cementitious composites: comparison of nanosilica and microsilica. Constr Build Mater. 2016;102:706–13. https://doi.org/10.1016/j.conbuildmat.2015.11.020.

22. Iravani S. Mechanical properties of high-performance concrete. Mater J. 1996;93(5):416–26.

23. Liu T, Wang Z, Zeng J, Wang J. Machine-learning-based models to predict shear transfer strength of concrete joints. Eng Struct. 2021;249: 113253. https://doi.org/10.1016/j.engstruct.2021.113253.

24. Mary Beth D, et al. Keating, Mechanical properties for High strength concrete for Pre-stressed members. ACI Struct J. 2004;101(4):457–66.

25. Mazloom M, Ramezanianpour AA, Brooks JJ. Effect of silica fume on mechanical properties of high-strength concrete. Cement Concr Compos. 2004;26(4):347–57.

26. Mane BV, Patil VS, Kulkarni S. Analysis of slender reinforced high performance concrete columns using ANSYS software. In AIP Conference Proceedings Vol. 2716, No. 1. AIP Publishing. 2023.

27. Ozturan. T, An investigation of concrete abrasion as two phase material, PhD thesis, Faculty of civil Engineering, Istambul Technical University, 1984.

28. Pul S. Experimental investigation of tensile behavior of high strength concrete. Indian J Eng Mater Sci. 2008;15:467–72.

29. Shafieifar M, Farzad M, Azizinamini A. Experimental and numerical study on mechanical properties of Ultra High Performance Concrete (UHPC). Constr Build Mater. 2017;156:402–11. https://doi.org/10.1016/j.conbuildmat.2017.08.170.

30. Shi T, Li Z, Guo J, Gong H, Gu C. Research progress on CNTs/CNFs-modified cement-based composites–a review. Constr Build Mater. 2019;202:290–307. https://doi.org/10.1016/j.conbuildmat.2019.01.024.

31. Soutsos, M. N., Breysse, D., Garnier, V., Goncalves, A., & Monteiro, A. V. (2012). Estimation of on-site compressive strength of concrete. Non-Destructive Assessment of Concrete Structures: Reliability and Limits of Single and Combined Techniques: State-of-the-Art Report of the RILEM Technical Committee 207-INR, 119–186.

32. Shanmugapriya T, Uma RN. Experimental investigation on silica fume as partial replacement of cement in high performance concrete. Int J Eng Sci. 2013;2(5):40–5.

33. Tayeh BA, Al Saffar DM, Alyousef R. The utilization of recycled aggregate in high performance concrete: a review. J Market Res. 2020;9(4):8469–81. https://doi.org/10.1016/j.jmrt.2020.05.126.

34. Turan A, Tunç AÖ, Zehir C. A theoretical model proposal: Personal innovativeness and user involvement as antecedents of unified theory of acceptance and use of technology. Procedia Soc Behav Sci. 2015;210:43–51. https://doi.org/10.1016/j.sbspro.2015.11.327.

35. Wee TH, Chin MS, Manasur MA. Stress-strain relationship of high-strength concrete in compression. J Mater Civil Eng. 1996;8:70–6.

36. Wang Y, Shi T, Fan QY, Liu Y, Zhang A, Li Z, Zeng S. Discovering surface structure and the mechanism of graphene oxide-triggered CeO2–WO3/TiO2 catalysts for NO abatement with NH3. ACS Catal. 2022;12(14):8386–403.

37. Wu Z, Wang X, Zhao X, Noori M. State-of-the-art review of FRP composites for major construction with high performance and longevity. Int J Sustain Mater Struct Syst. 2014;1(3):201–31. https://doi.org/10.1504/IJSMSS.2014.062757.